Optimization of load paths in X- and Y-shaped hydroforming

Mehran Kadkhodayan & Ahmad Erfani Moghadam

International Journal of Material Forming

ISSN 1960-6206

Int J Mater Form
DOI 10.1007/s12289-011-1074-3

Springer

Int J Mater Form
DOI 10.1007/s12289-011-1074-3

ORIGINAL RESEARCH

Optimization of load paths in X- and Y-shaped hydroforming

Mehran Kadkhodayan · Ahmad Erfani Moghadam

Received: 6 April 2011 / Accepted: 16 August 2011

Abstract An optimization of load paths in hydroforming of angled tubes are investigated through statistical methods in conjunction with FEA and simulated annealing algorithms. The main aim of this study is to improve the tube formability by applying the optimal load parameters. A new method to design the optimal load paths is represented and it is applied to optimize the load curves in hydroforming of X- and Y- tube shapes. By the aid of proposed method, the tube is formed with good formability indicators and lower capacity of equipments. Comparing the results of this study with the experimental data confirm the effectiveness of the method.

Keywords Hydroforming · Load paths · Angled tube · Design of experiment · FEA · ANOVA · SA

Introduction

Manufacturing of complicated components with high quality induce that the hydroforming process is became one of the main interest for researchers and manufactures. Angled hollow components such as X-, T- and Y-branches used in exhaust manifolds and piping systems are commonly manufactured by hydroforming process. There are many different variables in this process that have significant influences on the final quality of products, hence, manufacturing of different components without any defects such as bursting or wrinkling encounter with many difficulties. One of the most important parameters is the adjustment of loading variables which is called as "design of load paths" during the hydroforming process. Loading parameters in this process are included internal pressure and axial-punch displacement that should be determined associated with each other. Because of shortage in background of this process, many manufactures use specific load paths for the applications which have designed by trail and error method. Hence, to design the optimal load paths many researchers have concentrated on the optimization of design of load paths in hydroforming process. Ray [1, 2] investigated the manufacturing of T- and X-shapes joints by FE simulation and optimized the load paths by using of fuzzy load control algorithm. Kokanda [3] studied hydroforming of X-shape tube. Altan [4] investigated the effect of geometric parameters on the hydroforming of Y-shape tube. Ingarao [5] studied the effect of internal pressure and counter-punch loading parameters on the hydroforming of Y-shape tube. Teng [6] analyzed the thickness distribution of tube in Y-shape hydroforming.

In the current study, the optimization of load paths for hydroforming of angled tubes is represented. First, a summary of proposed optimization process is described. Then, the hydroforming of X- and Y-shapes tubes and their optimal load paths are studied and designed. The efficiency of the proposed method is investigated in detail.

Design of optimal load curves

In hydroforming process, tube is placed in a die and is formed by simultaneous applying of internal pressure and axial-punch feeding from both ends. Manufacturing of different parts in this method depends on the die shape, however, the general principles are similar to each other.

M. Kadkhodayan (✉) · A. E. Moghadam
Department of Mechanical Engineering,
Ferdowsi University of Mashhad,
Mashhad, Iran
e-mail: kadkhoda@um.ac.ir

Published online: 26 August 2011

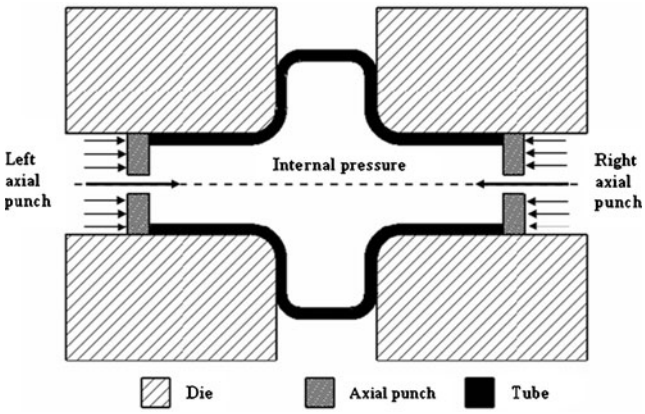

Fig. 1 The schematic view of X-shape hydroforming, geometry and load parameters

The schematic views of X- and Y-shapes tube hydroforming are shown in Figs. 1 and 2, respectively.

A proper adjustment of existing variables in experiments has a significant role to achieve desired products in the most engineering applications. For example, if there are seven variables in a process, and if two situations are considered for each variable, then 128 experiments should be carried out, which is unreasonable. By increasing the number of situations for each variable, the volume of experiments increases in an exponential form. Generally, design of experiment (DOE) is used to determine an appropriate set of experiments for a process in such a way that all situations can be covered with a reasonable number of experiments. To carry out a successful analysis with DOE, different components have to be chosen accurately consist of the input variables, the bounds and the number of levels of each input variable, the types of designed experiments and the output variables (response variables).

The input variables include all loading parameters and will be discussed later in this manuscript. According to the nature of process, the geometrical and material specifications for tools and tube, the suitable bounds and the number

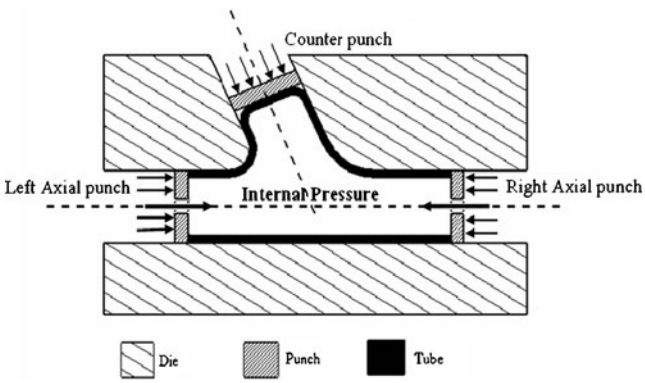

Fig. 2 The schematic diagram of Y-shape hydroforming process

Table 1 Mechanical properties of copper tube [1]

Factor	Value
Young modulus E (GPa)	119.86
Poisson coefficient (υ)	0.31
Yield stress (σ_y) (GPa)	0.116
Strength factor (K)(GPa)	0.4257
Strain hardening exponent (n)	0.2562
Density(kg/ m^3)	8900

of levels for each variable are chosen. There are four types of design of experiments including full factorial, response surface, mixture and Taguchi methods. In this study, the Taguchi method with the general form of $L_N(n^k)$ is chosen to determine the load paths, where L is the notation of Taguchi design, N is the number of experiments, n is the number of levels of each variable and k is the number of variables. With respect to the significance of the variables, the two and three levels approaches are considered that are discussed in the next parts.

The output or response variables are introduced as the best values to evaluate the tube formability according to the input variables (loading variables), that are determined based on the nature of process. When the appropriate experiments are designed the obtained data are embedded to FE software to analyze the whole process. In the current study, the Abaqus/Explicit is used to simulate the experiments. First, the experimental models of X- and Y-shapes hydroforming are verified. Then, the experiments designed by DOE are investigated and the desired outputs for each set of input variables are calculated. Finally, the statistical analysis is carried out on the Taguchi tables of X- and Y-shapes hydroforming processes.

By using of statistical analysis on the Taguchi table, it is possible to evaluate the tube formability according to the loading variables. In fact, the other situations of loading variables which are not included in FEA are studied. Determination of the tube formability indicators for different loading variables is carried out with the aid of regression analysis and statistical interpolation on obtained data. The dependent variables (formability indicators) are

Table 2 Comparison between the results of FEA and experimental model [1]

Maximum-internal pressure (GPa)	0.037
Maximum-feed (L) (mm)	18.5
Protrusion height (H) (mm) (experiment) [1]	14.75
Protrusion height (H) (mm) (simulation) [1]	15.44
Protrusion height (H) (mm) (simulation by Abaqus/Explicit)	14.94

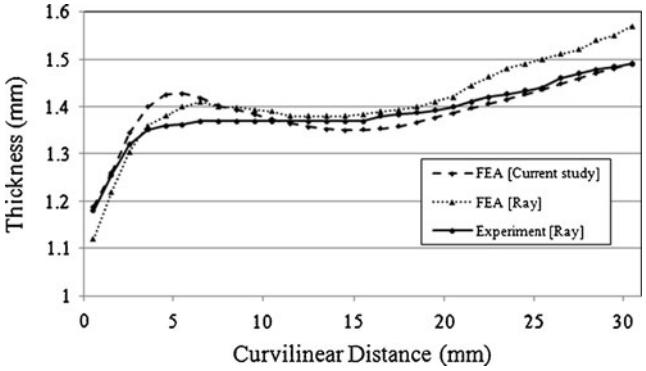

Fig. 3 Comparison of thickness in zx direction

calculated by mathematical functions consist of linear, curvilinear, exponential and stepwise from independent variables (loading variables). In this study, the regression analysis is carried out based on the mentioned functions except of curvilinear one because of its lower accuracy. A general form of the linear function is according to the following equation,

$$Y_i = \alpha_0 + \sum_{i=1}^{n} \alpha_i X_i \qquad i = 1\,,\,2\,,\,\ldots.,\,n \tag{1}$$

where Y_i indicates the output variables, α_0 is a constant, α_i are coefficients of the variables and X_i are the input variables. Respective coefficients are calculated by the least square method. If some variables do not have significant effect on the process, they can be eliminated to simplify the model. This kind of model is called stepwise and according to the regression models it may have linear or curvilinear form. In this study the linear stepwise model is used. The general form of an exponential model is as Eq. 2 and all parameters are the same as a linear function.

$$Y_i = \alpha_0 \prod_{i=1}^{n} X_i^{\alpha_i}, \quad i = 1\,,2,\ \ldots.,n \tag{2}$$

The regression models are calculated by using the statistical analysis in the Minitab software.

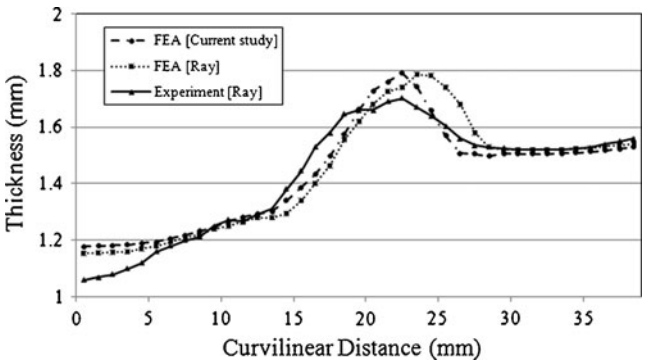

Fig. 4 Comparison of thickness in zy direction

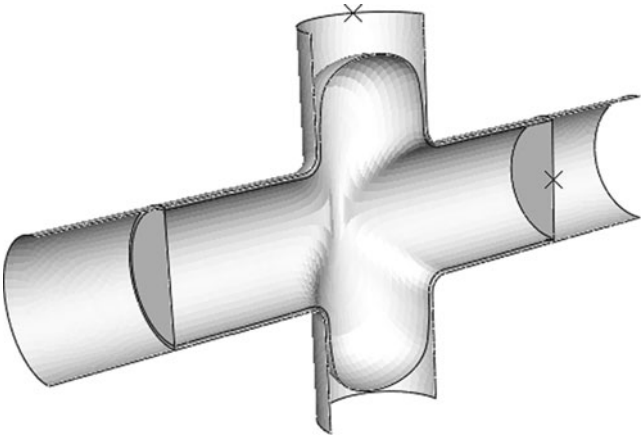

Fig. 5 Hydroformed tube at the end of simulation

As aforementioned, the regression models are used to estimate the tube formability. To find the most appropriate models, some criterions can be used as are mentioned below. The most important method to compare the regression models is calculation of correlation factors. This parameter is found according to the residual concept. If the value of this factor approaches to 100%, it means that the accuracy of the model is very good. However, it is not sufficient for the selection of the model and more requirements need to be met.

Another way to investigate the accuracy of a model is calculation of its residual distribution; i.e. a nonspecific shape of residual distribution means that the model has a good accuracy and vice versa [7].

The third method to investigate a represented model is carrying out the statistical tests. For instance, some sets of arbitrary variables are chosen and the results of tube formability are calculated and compared with those from FEA. Then, the error of each formability indicator is calculated and the best model is selected for inserting into the optimization algorithm.

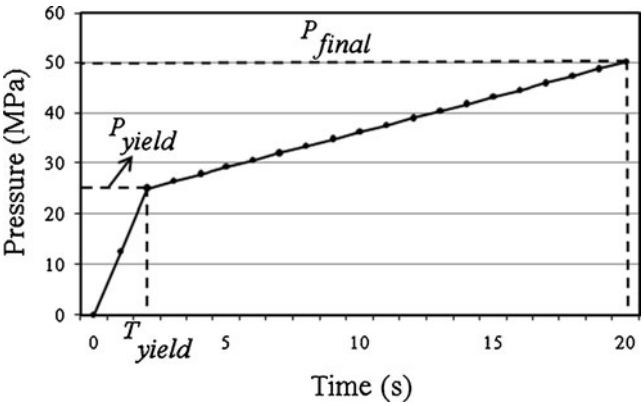

Fig. 6 General path of internal pressure

Table 3 The proposed levels of loading variables

No.	Factor	Notation	Unit	Levels	Value
1	Yield time	T_{yield}	s	−	2
				0	5
				+	8
2	Yield pressure	P_{yield}	MPa	−	10
				0	17.5
				+	25
3	Final pressure	P_{final}	MPa	−	30
				0	40
				+	50
4	Initial time of displacement	$T_{initial}$	s	−	4
				0	6
				+	8
5	Initial displacement	$S_{initial}$	mm	−	6
				0	9
				+	12
6	Middle time of displacement	T_{middle}	s	−	12
				+	16
7	Middle displacement	S_{middle}	mm	−	15
				0	20
				+	25
8	Final displacement	S_{final}	mm	−	25
				+	30

Analysis of variance (ANOVA) is a powerful technique in statistical analysis and gives us a good opportunity to investigate the effect of each input variable on the outputs; i.e. the effect of each load variable on the tube formability indicators. Based on this analysis, it is possible to choose more significant variables and decrease the complexity of the experimental setup of the process. The pairwise effect of load variables on the formability indicators can also be studied. Using ANOVA, it is possible to investigate the instantaneous effect of two variables on the outputs. It

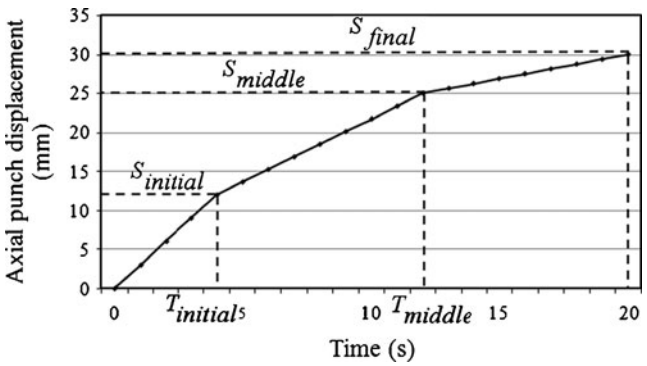

Fig. 7 General path of axial-punch displacement

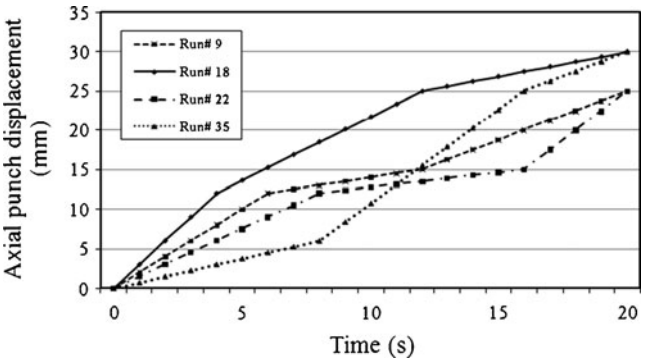

Fig. 8 Four paths of axial-punches

provides the possibility of studying the variations of outputs during the change of two loading variables.

Generally, adjustment of loading variables to design the load paths in X- and Y-shapes hydroforming is a complex and difficult task. Hence, an appropriate method should be applied to find the best loading variables to manufacture a product with a high quality. After applying all mathematical models, the optimum values for design of load curves are determined using an optimization algorithm. According to the essence of current problem, the simulated annealing (SA) algorithm is chosen for optimization algorithm. Simulated annealing algorithms are a family of computational models inspired by evolution and are often viewed as function optimizers. They are based on the concept of metallurgical annealing of solids and metals. In the annealing process, a solid is melted at high temperature until all molecules can move about freely. Then a cooling process is performed until thermal mobility is lost. The perfect crystal is the one in which all atoms are arranged in a low level lattice, therefore the crystal reaches the minimum energy [8–10].

Design of optimal load path in X-shape hydroforming

The design of optimal load paths for the X-shape hydroforming is investigated in this part. As prescribed before, the Abaqus/Explicit software is used to carry out the cases (experiments), however, it is needed first to verify the

Table 4 Tube formability indicators

No.	Factor	Notation	Unit
1	Minimum thickness at zx	$T_{min\ (zx)}$	mm
2	Minimum thickness at zy	$T_{min\ (zy)}$	mm
3	Maximum thickness at zy	$T_{max\ (zy)}$	mm
4	Maximum protrusion height	H_{max}	mm

Table 5 Results of experiments carried out by FEA

No.	T_{yield}	P_{yield}	P_{final}	$T_{initial}$	$S_{initial}$	T_{middle}	S_{middle}	S_{final}	$T_{min\ (zx)}$	$T_{min\ (zy)}$	$T_{max\ (zy)}$	H_{max}
1	−	−	−	−	−	−	−	−	1.319	1.512	1.772	18.81
2	0	0	0	0	0	−	0	−	1.314	1.433	1.631	19.82
3	+	+	+	+	+	−	+	−	1.301	1.200	1.634	19.80
4	−	−	−	−	0	−	0	−	1.318	1.315	2.050	13.61
5	0	0	0	0	+	−	+	−	1.315	1.306	1.887	16.25
6	+	+	+	+	−	−	−	−	1.271	1.124	1.486	22.24
7	−	−	0	+	−	−	0	−	1.281	1.378	1.595	20.54
8	0	0	+	−	0	−	+	−	1.288	1.075	1.758	18.53
9	+	+	−	0	+	−	−	−	1.322	1.289	1.960	18.37
10	−	−	+	0	−	−	+	+	1.277	1.228	1.620	24.53
11	0	0	−	+	0	−	−	+	1.310	1.339	1.764	23.56
12	+	+	0	−	+	−	0	+	1.325	1.154	1.901	18.32
13	−	0	+	−	+	−	0	+	1.284	1.007	1.555	25.72
14	0	+	−	0	−	−	+	+	1.312	1.394	1.622	23.94
15	+	−	0	+	0	−	−	+	1.305	1.446	2.041	17.60
16	−	0	+	0	−	−	−	+	1.245	0.980	1.515	27.86
17	0	+	−	+	0	−	0	+	1.283	1.195	1.710	24.14
18	+	−	0	−	+	−	+	+	1.361	1.412	1.968	8.94
19	−	0	−	+	+	+	+	−	1.283	1.424	1.657	19.91
20	0	+	0	−	−	+	−	−	1.297	1.135	1.487	21.72
21	+	−	+	0	0	+	0	−	1.286	1.329	1.927	15.13
22	−	0	0	+	+	+	−	−	1.260	1.178	1.503	21.65
23	0	+	+	−	−	+	0	−	1.280	1.090	1.451	22.64
24	+	−	−	0	0	+	+	−	1.328	1.540	2.142	10.30
25	−	+	0	−	0	+	+	−	1.268	1.176	1.492	21.76
26	0	−	+	0	+	+	−	−	1.278	0.948	2.009	19.59
27	+	0	−	+	−	+	0	−	1.311	1.466	1.681	19.49
28	−	+	0	0	0	+	−	+	1.250	0.991	1.565	26.83
29	0	−	+	+	+	+	0	+	1.283	1.066	1.907	24.06
30	+	0	−	−	−	+	+	+	1.341	1.468	1.941	16.75
31	−	+	+	+	0	+	+	+	1.221	0.906	1.512	28.69
32	0	−	−	−	+	+	−	+	1.344	1.374	1.914	14.49
33	+	0	0	0	−	+	0	+	1.312	1.320	1.656	24.27
34	−	+	−	0	+	+	0	+	1.267	1.133	1.702	24.64
35	0	−	0	+	−	+	+	+	1.291	1.342	1.714	23.90
36	+	0	+	−	0	+	−	+	1.280	0.971	1.950	23.22

simulation model with an experimental model. To do this, the experimental set studied by Ray [1] is selected and a tube with a length of 121 mm, an output diameter of 24 mm and a thickness of 1.3 mm is analyzed. Tube properties are listed in Table 1. Similar to the reference, tube is considered to be isotropic and similar load paths are applied on the tube. The calculated results obtained from applying of similar load paths are compared with those of experimental results in Table 2 and the thickness distribution in both zx and zy planes are seen in Figs. 3 and 4, respectively. The final shape of formed tube is shown in Fig. 5. Two load parameters in X-shape hydroforming consist of internal pressure and axial-punches displacement are discussed in detail in the following.

Table 6 Correlation factors of different models

Model	$T_{min\ (zx)}$	$T_{min\ (zy)}$	$T_{max\ (zy)}$	H_{max}
Linear	90.1%	86.8%	79.1%	89.0%
Stepwise	90.02%	86.25%	78.56%	88.96%
Exponential	90.5%	83.1%	81.5%	81.4%

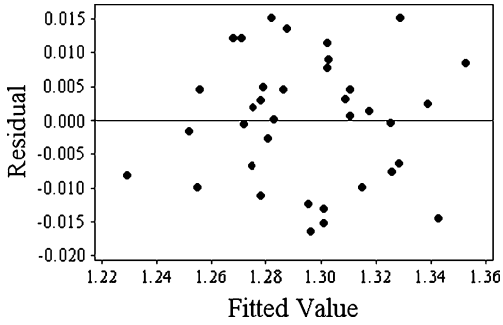

Fig. 9 Residual distribution of $T_{min\ (zx)}$ for linear model

Determination of an appropriate pressure function during the hydroforming process is a crucial factor in design of load curves. There are different curves for pressure which can be categorized in two general paths as linear and pulsating forms. In the current study the linear form of internal pressure is selected. There is a general path for internal pressure proposed by Altan [10] and Hwang [11] which used in the current study. Five variables for design of pressure path are initially assumed, but statistical investigations reveal that the expansion pressure does not have significant effect on the tube formability. Therefore, to investigate the process more accurately it is removed from the list of design variables. A pressure path based on three variables consist of yield pressure, its respective time and final pressure is indicated in Fig. 6. All variables with their notations are listed in Table 3.

This is clear that if only the internal pressure is applied in hydroforming process it causes excessive thinning in tube. Therefore, to avoid extra thinning two axial-punches are used to feed both ends of tube into die. Because of the symmetry, both paths for axial-punches are similar and only one path may be investigated. Although two stages displacement path is common to be used [12–14], statistical analysis indicated that a three stages path perform more proper forming. Hence, the general path of axial-punch is assumed to be as Fig. 7 and the respective variables are listed in Table 3. Appropriate bounds for each variable are determined according to experimental models, different FE simulations, analytical relations for pressure and some experimental observations, Table 3.

The Taguchi design of $L_{36}(2^2\times3^6)$ is carried out using Table 3. In this design the maximum number of experiments is considered and applied to DOE portion of statistical software Minitab, Table 5. Using this table, each load path is designed as illustrated for four samples of axial-punch paths in Fig. 8. Based on the nature of X-shape hydroforming, the output variables (described earlier) are determined. The minimum thickness is usually occurred in zy plane. Hence, both minimum and maximum thicknesses in this plane are considered as tube indicators. On the other hand, the minimum thickness in zx plane along with the maximum height of protrusion are taken as indicators. The four mentioned indices are calculated by applying each set of load paths on the experimental model, Table 4. Each experiment is carried out by Abaqus/Explicit 6.7 and the four indices are calculated after the end of each simulation, Table 5.

Now, based on the regression analysis in Minitab software, three different models are considered.

1- Linear model

$$T_{min(zx)} = 1.43 + 0.00653\ T_{yield} - 0.00152\ P_{yield} - 0.00185\ P_{final} - 0.00635\ T_{initial} + 0.00119\ S_{initial} - 0.00349\ T_{middle} + 0.000875\ S_{middle} - 0.000322\ S_{final} \quad (3)$$

$$T_{min(zy)} = 2.35 + 0.0207\ T_{yield} - 0.0117\ P_{yield} - 0.0147\ P_{final} + 0.00781\ T_{initial} - 0.0131\ S_{initial} - 0.0129\ T_{middle} + 0.00987\ S_{middle} - 0.0132\ S_{final} \quad (4)$$

Table 7 Tube formability indicators versus linear model and their respective differences (errors) with FE analysis

No.	Linear model results				Difference between the linear model and FEA			
	$T_{min\ (zx)}$	$T_{min\ (zy)}$	$T_{max\ (zy)}$	H_{max}	$T_{min\ (zx)}$	$T_{min\ (zy)}$	$T_{max\ (zy)}$	H_{max}
1	1.28	1.17	1.69	23.15	1.73	5.29	6.58	4.19
2	1.31	1.40	1.73	17.95	0.01	1.94	1.24	6.36
3	1.30	1.23	1.82	19.09	0.80	5.02	6.47	5.27
4	1.31	1.22	1.78	19.51	0.88	2.06	5.37	7.66
5	1.26	1.12	1.58	23.38	1.69	0.88	6.23	3.35

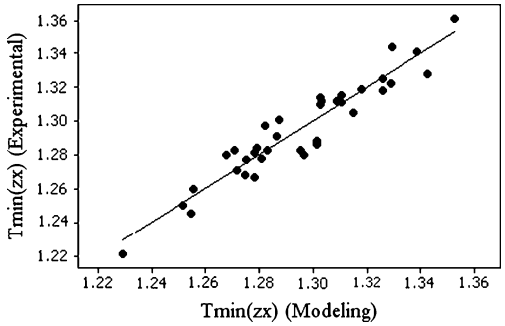

Fig. 10 The scatter plot of minimum thickness at the zx direction

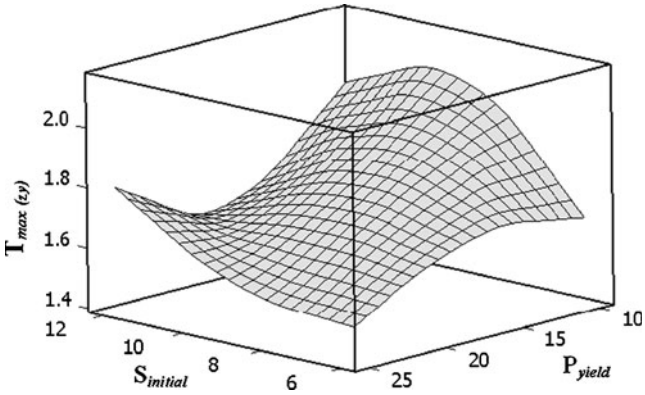

Fig. 12 The pairwise effect of initial displacement of axial-punch ($S_{initial}$) and yield pressure (P_{yield}) on the maximum thickness at zy direction

$$T_{max(zy)} = 1.91 + 0.0382\ T_{yield} - 0.0174\ P_{yield} - 0.00663\ P_{final} - 0.0216\ T_{initial} + 0.0286\ S_{initial} - 0.00360\ T_{middle} - 0.00016\ S_{middle} + 0.00483\ S_{final} \quad (5)$$

$$H_{max} = -7.47 - 0.835\ T_{yield} + 0.342\ P_{yield} + 0.183\ P_{final} + 0.856\ T_{initial} - 0.485\ S_{initial} + 0.229\ T_{middle} - 0.189\ S_{middle} + 0.681\ S_{final} \quad (6)$$

2- Linear stepwise model

$$T_{min(zx)} = 1.421 + 0.00653\ T_{yield} - 0.00152\ P_{yield} - 0.00185\ P_{final} - 0.0064\ T_{initial} + 0.00119\ S_{initial} - 0.00349\ T_{middle} + 0.00087\ S_{middle} \quad (7)$$

$$T_{min(zy)} = 2.395 + 0.0207\ T_{yield} - 0.0117\ P_{yield} - 0.0147\ P_{final} - 0.0131\ S_{initial} - 0.0129\ T_{middle} + 0.0099\ S_{middle} - 0.0132\ S_{final} \quad (8)$$

Fig. 11 The percentage effect of loading variables on the height

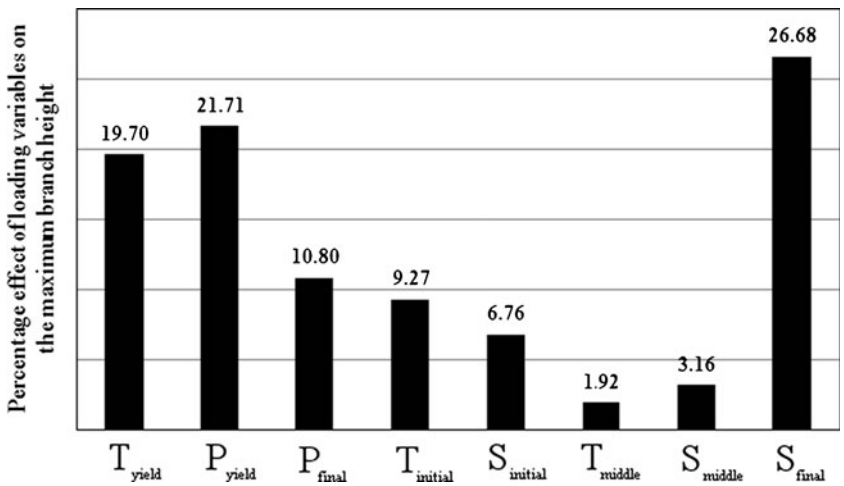

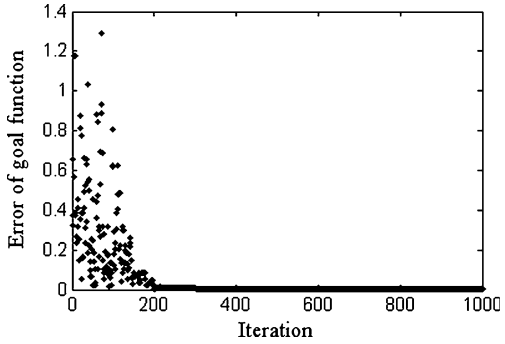

Fig. 13 The convergence rates for SA algorithm

$$T_{max(zy)} = 1.993 + 0.0382\ T_{yield} - 0.0174\ P_{yield} - 0.0066\ P_{final} - 0.022\ T_{initial} + 0.0286\ T_{middle} \quad (9)$$

$$H_{max} = -7.47 - 0.83\ T_{yield} + 0.342\ P_{yield} + 0.183\ P_{final} + 0.86\ T_{initial} - 0.49\ S_{initial} + 0.23\ T_{middle} - 0.189\ S_{middle} + 0.68\ S_{final} \quad (10)$$

3- Exponential model

$$T_{min(zx)} = 10^{0.262}(T_{yield}{}^{0.0220})(P_{yield}{}^{-0.0189})(P_{final}{}^{-0.0550})(T_{initial}{}^{-0.0284})(S_{initial}{}^{0.00644})(T_{middle}{}^{-.0377})(S_{middle}{}^{0.0131})(S_{final}{}^{-0.0083}) \quad (11)$$

$$T_{min(zy)} = 10^{1.45}(T_{yield}{}^{0.0701})(P_{yield}{}^{-0.148})(P_{final}{}^{-0.467})(T_{initial}{}^{0.375})(S_{initial}{}^{-0.093})(T_{middle}{}^{-0.164})(S_{middle}{}^{0.162})(S_{final}{}^{-0.311}) \quad (12)$$

$$T_{max(zy)} = 10^{0.449}(T_{yield}{}^{0.0908})(P_{yield}{}^{-0.165})(P_{final}{}^{-0.158})(T_{initial}{}^{-0.0630})(S_{initial}{}^{0.148})(T_{middle}{}^{-0.0360})(S_{middle}{}^{0.0006})(S_{final}{}^{0.0916}) \quad (13)$$

$$H_{max} = 10^{-0.615}(T_{yield}{}^{-0.178})(P_{yield}{}^{0.327})(P_{final}{}^{0.368})(T_{initial}{}^{0.282})(S_{initial}{}^{-0.242})(T_{middle}{}^{0.164})(S_{middle}{}^{-0.240})(S_{final}{}^{0.821}) \quad (14)$$

Table 9 Tube formability results versus optimal loading variables by FEA

No.	$T_{min\ (zx)}$	$T_{min\ (zy)}$	$T_{max\ (zy)}$	H_{max}
1	1.235	1.027	1.566	25.6
2	1.23	1.051	1.678	25.54
3	1.245	1.169	1.541	22.31
4	1.238	1.193	1.518	21.87
5	1.23	1.16	1.537	23.01

Now the prescribed methods to choose the best models are investigated. The correlation factors for all models and outputs are listed in Table 6 and as it is seen, all models have proper accuracy. The residual distributions for $T_{min(zx)}$ are shown in Fig. 9. The distribution of residuals has no specific shape which is a necessary condition for an acceptable distribution. It is possible to show all residual distributions for each output, however, for the sake of abbreviation only one residual distribution is illustrated.

Based on the carried out analyses, the linear model shows a better accuracy in this study. Hence, at first and to illustrate the reliability, five sets of input variables are chosen for each load variables and each experiment is analyzed by Abaqus/Explicit. Then, the obtained results are compared with those from mathematical models. The output indicators from linear model and their differences with FEA are tabulated in Table 7. The results show that the linear model can estimate the tube formability in a good accuracy and thus may be chosen to optimize the loading variables. To assert the adequacy of the linear model it is possible to compare the experimental results with the statistical analysis obtained by the scatter plot of data. The Fig. 10 shows the $T_{min\ (zx)}$ scatter of data and the prepared mathematical models have good conformability as mentioned before.

There are four outputs or tube formability indicators. With the aid of analysis of variance (ANOVA) on the values of Table 7, the influence of each load variable on the forming are investigated, Fig. 11. It is apparent that for each output the effect of loading variables are different, hence it is possible to remove the variables with low effect to decline the complexity of the problem. Using ANOVA it is also possible to investigate the instantaneous effect of two

Table 8 Optimal loading variables calculated by SA algorithm

No.	T_{yield}	P_{yield}	P_{final}	$T_{initial}$	$S_{initial}$	T_{middle}	S_{middle}	S_{final}
1	2.4	23.8	38.4	7.3	6.1	15.5	21.6	28.7
2	2.1	24.4	33.4	7.2	6.4	12.9	24.5	30
3	3	23.7	33.2	7.4	6.1	16	24.6	25.8
4	2.2	22.9	34	7	6.1	12.1	18.2	25.2
5	2	23.9	34.8	6.8	6.1	12.8	22.1	26.4

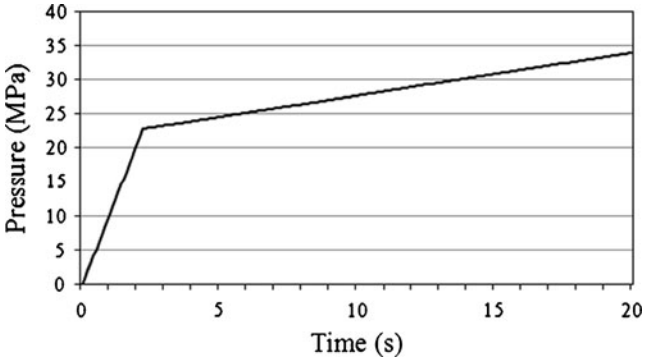

Fig. 14 The optimal path of internal pressure

variables on the outputs, which provides the possibility of variation of output during the changing of two loading variables. The pairwise effect of loading variables for $T_{max\ (zy)}$ is shown in Fig. 12.

In the optimization process an objective function is determined with a kind of error function. For a linear model this function is constructed as follows,

$$F = \frac{\left(T_{min(zx)\,exp} - T_{min(zx)}\right)^2}{T_{min(zx)\,exp}} + \frac{\left(T_{min(zy)\,exp} - T_{min(zy)}\right)^2}{T_{min(zy)\,exp}} + \frac{\left(T_{max(zy)\,exp} - T_{max(zy)}\right)^2}{T_{max(zy)\,exp}} + \frac{\left(H_{exp} - H\right)^2}{H_{exp}} = 0 \quad (15)$$

In this equation, $T_{min\ (zx)\ exp}$, $T_{min\ (zy)\ exp}$, $T_{max\ (zy)\ exp}$ and H_{exp} are substituted according to the Eqs. 5–8 and $T_{min\ (zx)}$, $T_{min\ (zy)}$, $T_{max\ (zy)}$ and H are the proper values chosen based on the geometrical specifications and designing point of views. By applying the respective relations and values on the Eq. 17, the SA algorithm is constructed in MATLAB software. The convergence rate of this algorithm to optimize the load paths is shown in Fig. 13. It is seen that the convergence rate for this problem is quite high and after 300 iterations the algorithm is converged into the proper answer. Five sets of optimal values for loading variables are calculated and

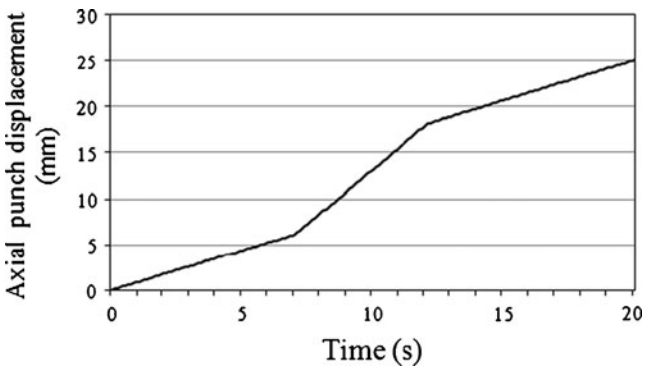

Fig. 15 The optimal path of axial-punch displacement

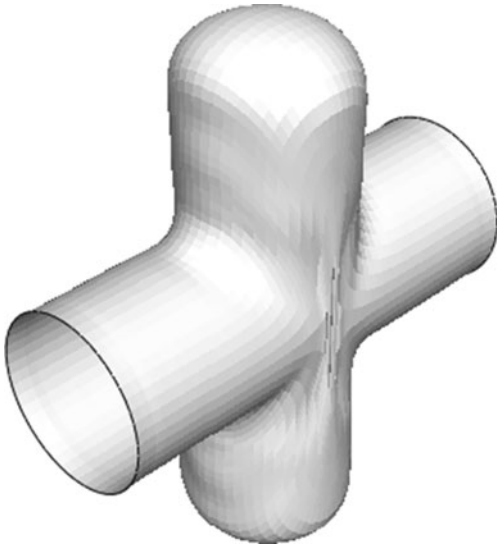

Fig. 16 Hydroformed tube by applying of optimal load path

inserted in Table 8. The effect of each load path on the tube hydroforming is studied by FEM and the obtained results are listed in Table 9. Usually and for the common applications, it is preferred to have a joint with higher protrusion and minimum deviation of thickness. Therefore, the fourth set of data is chosen as the best results. The corresponding loading paths for internal pressure and axial-punch are shown in Figs. 14 and 15, respectively. By applying above load paths to hydroforming of X-shape, a joint without any defects like the one is shown in Fig. 16 is resulted.

There are some criteria to study the efficiency of optimal load paths including maximum internal pressure, minimum thickness and maximum protrusion height. The efficiency of the optimal load paths is investigated via comparing with Ray results [1]. The final pressure in Ray model is 37 MPa, while the obtained optimum value in this study is 34 MPa. Moreover, the height of protrusions in Ray model and in the current study are 14.94 mm and 21.87 mm, respectively, that shows a significant improvement. Furthermore, the minimum thicknesses of the reference and the new obtained one are 1.18 and 1.193 mm, respectively, that it has also been improved slightly.

Table 10 Mechanical properties of copper tube [10]

Factor	Value
Young modulus E (GPa)	250
Poisson coefficient (υ)	0.3
Yield stress (σ_y) (MPa)	285
Strength factor (K)(GPa)	1.471
Strain hardening exponent (n)	0.584
Density(kg/ m^3)	8000

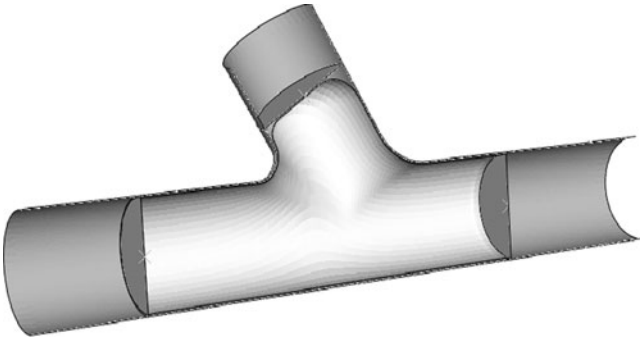

Fig. 17 Final shape of hydroforming process for tube and tools

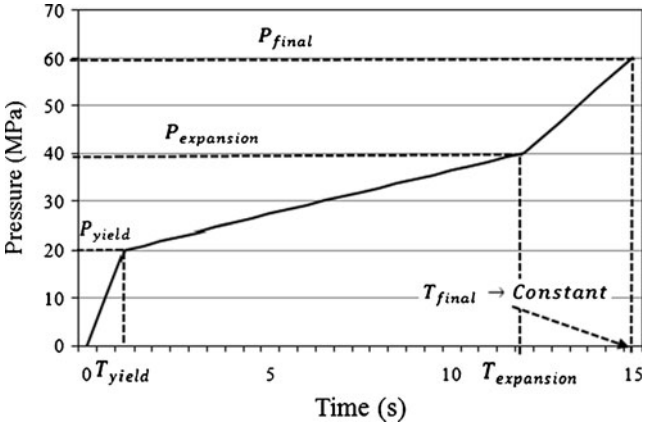

Fig. 19 General form of pressure path along with design variables

Design of optimal load path in Y-shape hydroforming

The Y-shape model studied by Altan [10] is chosen here for studying of load paths effect. The material properties of SS304 tube as shown in Table 10 are used in the FE model. By applying of respective load paths, the hydroforming process is carried out and the final shape of tube is shown in Fig. 17. Thickness distribution of the middle line is drawn in Fig. 18 to compare the simulation model with the experimental results and as it is seen they are in a good agreement.

A general form of path of internal pressure is shown in Fig. 19. The figure shows that there are different variables for designing this path contain yield pressure, time of yield pressure, bursting pressure, time of bursting pressure and final pressure as they are listed in Table 11. Based on the experimental results and some carried out simulations, it found that the time of yield pressure can be considered constant.

The Y-shape hydroforming is a non-symmetrical process, thus the movement paths of axial-punches are different and have to be designed autonomously. For the left axial-punch, three variables are considered consist of the displacement up to middle stage and its time and the final displacement of punch. A general form of its path of is shown in Fig. 20 and its respective variables are listed in Table 11. Similar variables are considered for the left punch. The right-axial punch path is plotted in Fig. 21 and its respective variables are listed in Table 11.

Generally it is possible to prevent excessive thinning in protrusion part by the aid of counter-punch. To design the counter-punch path, some variables have to be determined consist of starting time of counter-punch movement, initial place of counter-punch, its final place and the stopping time of movement. These variables are shown in Fig. 22 and are listed in Table 11 with their respective notations.

In the current study, the bounds of variables are chosen according to the experimental models and some FE simulations. Here, the method of determination of upper and lower bounds for right axial-punch variables is described briefly. Based on the experimental model [10], the lower bound for final feeding is fixed on 80 mm. For the upper bound, however, this magnitude is taken 110 mm initially. By applying this value to the right axial-punch wrinkling occurs in tube, see Fig. 23. Hence, an appropriate value for it is found as 100 mm. Similarly, an initial value for T_{ram} is considered as 8 s which

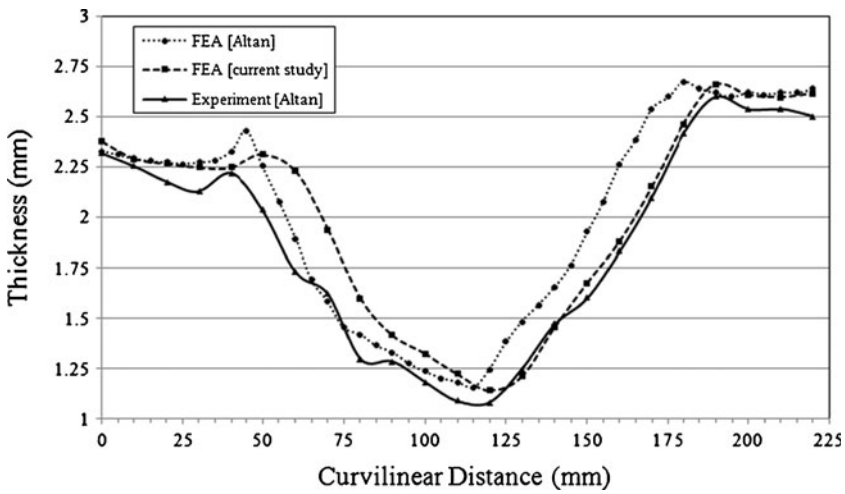

Fig. 18 Comparison of thickness distribution in the midline of hydroformed tube

causes wrinkling in the tube according to Fig. 24. It makes the final shape of tube as it is seen in Fig. 25. Hence, a suitable value for this parameter is found as 9 s. Similar ways are used to design the appropriate bounds for the rest of loading variables as are listed in Table 11.

Table 11 The upper and lower bounds for each loading variables

No.	Factor	Notation	Unit	Level	Value
1	Yield pressure	P_{yield}	MPa	−	7.5
				+	15
2	Expansion pressure	$P_{expansion}$	MPa	−	30
				0	35
				+	40
3	Expansion time	$T_{expansion}$	s	−	8
				+	11
4	Final pressure	P_{final}^{*}	MPa	−	40
				0	50
				+	60
5	Displacement of middle stage	S_{lap}	mm	−	9
				+	12
6	Time of middle stage	T_{lam}	s	−	30
				+	40
7	Final displacement of punch	S_{laf}	mm	−	40
				0	45
				+	50
8	Displacement of middle stage	S_{rap}	mm	−	9
				+	12
9	Time of middle stage	T_{ram}	s	−	60
				0	70
				+	80
10	Final displacement of punch	S_{raf}	mm	−	80
				0	90
				+	100
11	First place of counter-punch	T_{start}	s	−	4
				0	5
				+	6
12	End place of counter-punch	T_{stop}	s	−	11
				+	15
13	Starting time of movement	CP_s	mm	−	52
				+	56
14	Stopping time of movement	CP_f	mm	−	65
				0	70
				+	75

* Hint: Based on the experimental model, the value of final pressure is considered between 80-100 MPa, but according to the simulation results and experimental result, by using of this value excessive thinning occurred in tube. By carrying out different simulations, appropriate bound for final pressure is chosen between 40 and 60 MPa and according to this bounds for the internal pressure, the variables are modified.

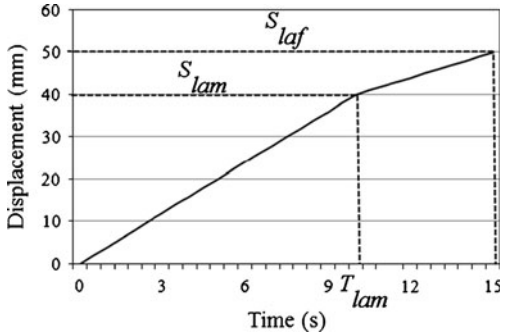

Fig. 20 General path of left axial-punch along with design variables

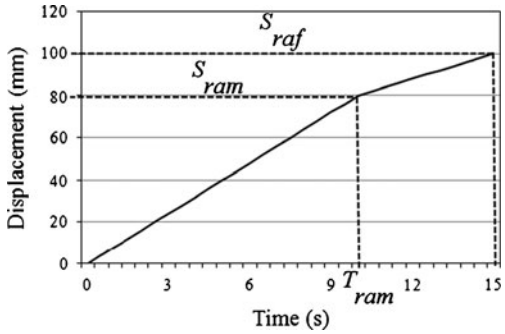

Fig. 21 The right axial-punch path

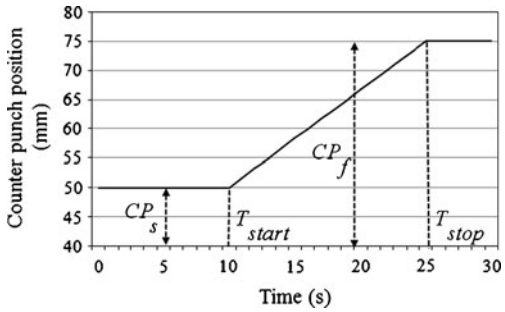

Fig. 22 Counter-punch path along with design variables

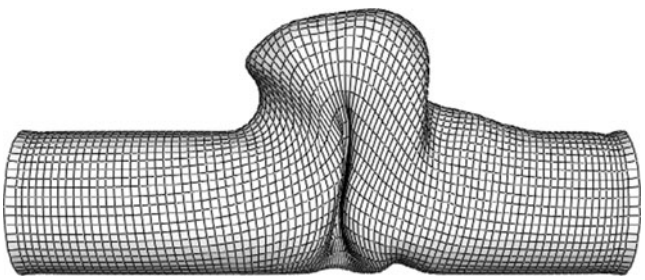

Fig. 23 Wrinkling occured in result of excessive feeding of right axial-punch

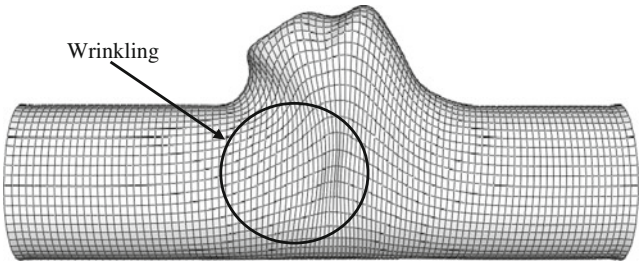

Fig. 24 Onset of wrinkling because of improper value of T_{ram}

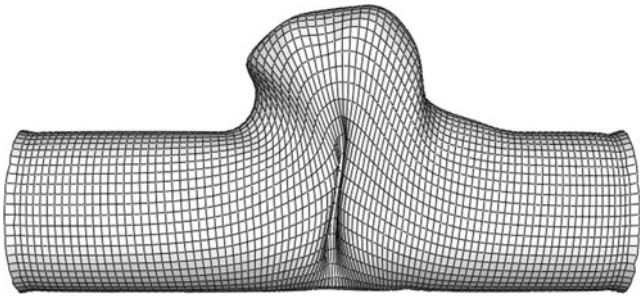

Fig. 25 Final shape of tube by applying of improper load paths

For seven variables with 2-levels and seven variables with 3-levels, the Taguchi design becomes according to $L_N(2^7 \times 3^7)$ and the number of total experiments will be 36. Therefore, thirty six experiments are designed by $L_{36}(2^7 \times 3^7)$ as are listed in Table 12. Using this table, it is possible to design each path of load parameter. It is shown for some experiments in Fig. 26 for the internal pressure.

In the most studies, the minimum thickness and protrusion height are considered for predefined purpose. In the current study also to investigate the load path effects these two parameters are established as outputs or dependent variables. The notations T and H stand for the minimum thickness and protrusion height, respectively. After applying each set of load paths, these two parameters are calculated as indicators of tube formability.

Now each set of load paths is applied to the hydroforming model and simulated by Abaqus/Explicit. Two indices of formability are obtained at the end of FEA and are listed for some experiments in Table 12. The regression models in this study are calculated by using of statistical analysis in Minitab software as follows,

1- Linear model

$$\begin{aligned}\text{Thickness} = {} & 1.57 - 0.00104\ P_{yield} + 0.00711\ T_{burst} - 0.00172\ P_{burst} - \\ & 0.00298\ P_{final} + 0.00089\ T_{lam} + 0.00231\ S_{lam} + 0.000433\ S_{laf} - \\ & 0.00267\ T_{rap} + 0.00111\ S_{ram} - 0.000242\ S_{raf} - 0.017\ T_{cps} - 0.0087\ T_{cpf} + 0.0393\ CP_s + 0.247\ CP_f\end{aligned} \tag{16}$$

$$\begin{aligned}\text{Height} = {} & -16.6 + 0.249\ P_{yield} - 0.474\ T_{burst} + 0.149\ P_{burst} + 0.0757\ P_{final} + \\ & 0.089\ T_{lam} - 0.0923\ S_{lam} + 0.140\ S_{laf} + 0.552\ T_{rap} - 0.124\ S_{ram} + \\ & 0.382\ S_{raf} - 0.017\ T_{cps} - 0.0087\ T_{cpf} + 0.0393\ CP_s + 0.247\ CP_f\end{aligned} \tag{17}$$

2- Stepwise model

$$\begin{aligned}\text{Thickness} = {} & 1.457 + 0.0071\ T_{burst} - 0.00172\ P_{burst} - 0.00298\ P_{final} + \\ & 0.00231\ S_{lam} + 0.00111\ S_{ram} - 0.00621\ T_{cps} + 0.00342\ T_{cpf} - 0.00152\ CP_f\end{aligned} \tag{18}$$

$$\begin{aligned}\text{Height} = {} & -13.772 + 0.249\ P_{yield} - 0.474\ T_{burst} + 0.149\ P_{burst} + 0.0757\ P_{final} - 0.0923\ S_{lam} + 0.141\ S_{laf} + 0.552\ T_{rap} - \\ & 0.124\ S_{ram} + 0.382\ S_{raf} + 0.247\ CP_f\end{aligned} \tag{19}$$

3- Exponential model

$$\begin{aligned}\text{Thickness} = {} & 10^{0.398}\ P_{yield}^{-0.00777}\ T_{burst}^{0.0482}\ P_{burst}^{-0.042}\ P_{final}^{-0.106}\ T_{lam}^{0.007} \\ & S_{lam}^{0.0579}\ S_{laf}^{0.014}\ T_{rap}^{-0.0214}\ S_{ram}^{0.0541}\ S_{raf}^{-0.0146}\ T_{cps}^{-0.0229}\ T_{cpf}^{0.0319} \\ & CP_s^{-0.0541}\ CP_f^{-0.0797}\end{aligned} \tag{20}$$

$$\begin{aligned}\text{Height} = {} & 10^{-0.835}\ P_{yield}^{0.0611}\ T_{burst}^{-0.1}\ P_{burst}^{0.121}\ P_{final}^{0.0816}\ T_{lam}^{0.0234} \\ & S_{lam}^{-0.0719}\ S_{laf}^{0.143}\ T_{rap}^{0.125}\ S_{ram}^{-0.191}\ S_{raf}^{0.762}\ T_{cps}^{0.0015}\ T_{cpf}^{-0.0037} \\ & CP_s^{0.056}\ CP_f^{0.376}\end{aligned} \tag{21}$$

Table 12 Taguchi design and obtained outputs

No.	P_{yield}	T_{burst}	P_{burst}	P_{final}	T_{lap}	S_{lam}	S_{laf}	T_{rap}	S_{ram}	S_{raf}	T_{cps}	T_{cpf}	CP_s	CP_f	T (mm)	H (mm)
1	−	−	−	−	−	−	−	−	−	−	−	−	−	−	1.389	38.86
2	−	−	0	0	−	−	0	−	0	0	0	−	−	0	1.341	45.13
3	−	−	+	+	−	−	+	−	+	+	+	−	−	+	1.325	49.45
4	−	−	−	−	−	−	−	−	−	0	0	+	+	0	1.401	43.56
5	−	−	0	0	−	−	0	−	0	+	+	+	+	+	1.372	49.83
6	−	−	+	+	−	−	+	−	+	−	−	+	+	−	1.365	41.36
7	−	−	−	−	+	+	0	+	+	−	0	−	−	+	1.422	39.53
8	−	−	0	0	+	+	+	+	−	0	+	−	−	−	1.384	47.17
9	−	−	+	+	+	+	−	+	0	+	−	−	−	0	1.322	51.85
10	−	+	−	−	−	+	+	+	0	−	+	+	−	0	1.474	40.00
11	−	+	0	0	−	+	−	+	+	0	−	+	−	+	1.44	42.37
12	−	+	+	+	−	+	0	+	−	+	0	+	−	−	1.356	48.11
13	−	+	−	0	+	−	+	+	−	+	0	−	+	−	1.397	48.50
14	−	+	0	+	+	−	−	+	0	−	+	−	+	0	1.304	41.85
15	−	+	+	−	+	−	0	+	+	0	−	−	+	+	1.412	45.02
16	−	+	−	0	+	+	+	−	0	−	−	+	+	+	1.394	39.61
17	−	+	0	+	+	+	−	−	+	0	0	+	+	−	1.43	39.84
18	−	+	+	−	+	+	0	−	−	+	+	+	+	0	1.403	48.76
19	+	−	−	0	+	+	−	−	+	+	+	+	−	−	1.41	45.12
20	+	−	0	+	+	+	0	−	−	−	−	+	−	0	1.376	43.66
21	+	−	+	−	+	+	+	−	0	0	0	+	−	+	1.391	48.14
22	+	−	−	0	+	−	0	+	+	+	−	+	+	0	1.383	50.67
23	+	−	0	+	+	−	+	+	−	−	0	+	+	+	1.316	48.78
24	+	−	+	−	+	−	−	+	0	0	+	+	+	−	1.366	46.10
25	+	−	−	+	−	+	0	+	−	0	+	−	+	+	1.317	50.28
26	+	−	0	−	−	+	+	+	0	+	−	−	+	−	1.408	47.75
27	+	−	+	0	−	+	−	+	+	−	0	−	+	0	1.381	43.16
28	+	+	−	+	+	−	0	−	0	0	−	−	−	−	1.381	44.19
29	+	+	0	−	+	−	+	−	+	+	0	−	−	0	1.42	49.15
30	+	+	+	0	+	−	−	−	−	−	+	−	−	+	1.374	42.08
31	+	+	−	+	−	+	+	−	+	0	+	−	+	0	1.363	43.83
32	+	+	0	−	−	+	−	−	−	+	−	−	+	+	1.408	49.93
33	+	+	+	0	−	+	0	−	0	−	0	−	+	−	1.39	40.20
34	+	+	−	+	−	−	−	+	0	+	0	+	−	+	1.33	51.77
35	+	+	0	−	−	−	0	+	+	−	+	+	−	−	1.407	40.01
36	+	+	+	0	−	−	+	+	−	0	−	+	−	0	1.37	49.61

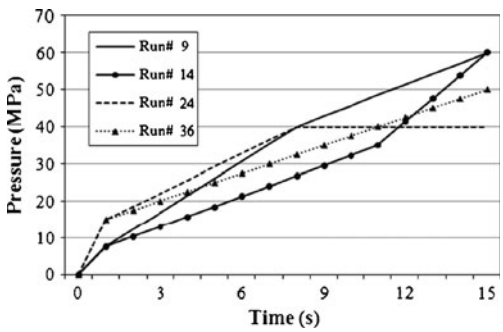

Fig. 26 Four sample paths of internal pressure

Table 13 Correlation factors of proposed models

Model	Thickness	Height
Linear	81.4%	95.8%
Stepwise	77.96%	95.67%
Exponential	80.2%	94.3%

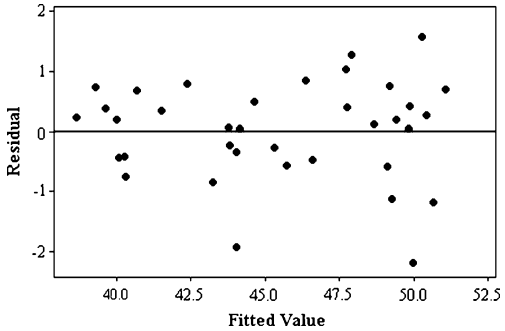

Fig. 27 The residuals versus fitted values for height

Table 14 The difference (error) between the FEA and proposed models.

No.	Linear and FEA		Stepwise and FEA		Exponential and FEA	
	T	H	T	H	T	H
1	0.364	0.509	0.337	0.548	0.186	0.072
2	0.529	1.150	1.160	1.261	0.720	0.998
3	0.497	1.218	0.187	0.951	0.170	1.087
4	0.571	0.917	0.627	0.910	0.251	0.830
5	1.215	0.163	1.453	0.276	1.395	0.335

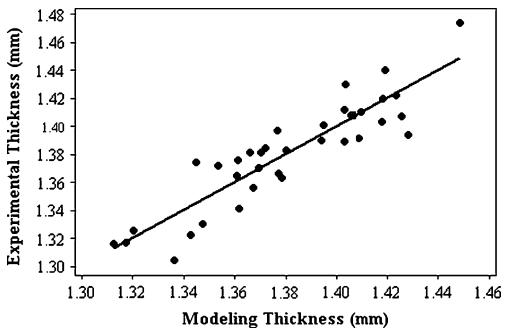

Fig. 28 The scatter plot for thickness

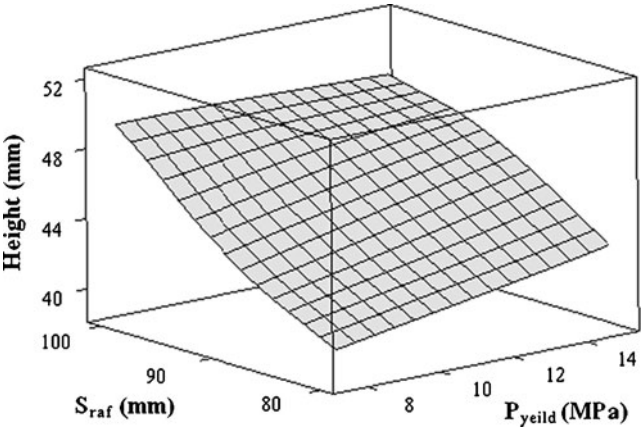

Fig. 30 The pairwise effect of S_{raf} and P_{yield} on the protrusion height

The correlation factors for proposed models are listed in Table 13. The results show that the linear models have an appropriate accuracy for estimation of both outputs. After choosing the linear models for estimation of tube formability, the assumption of independency of residuals is checked. The distribution of residuals of protrusion height is shown in Fig. 27. It is

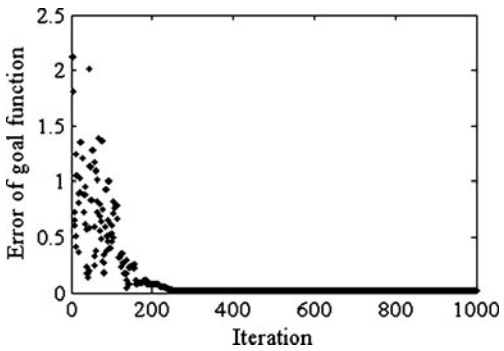

Fig. 31 The convergence rates for SA algorithm

Fig. 29 The effect of loading variables on the protrusion height

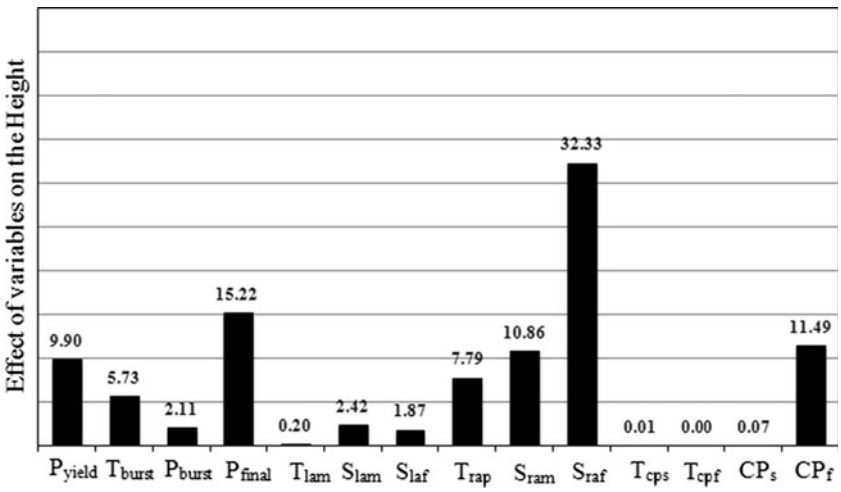

Table 15 Five sets of optimum values of loading variables

No.	P_{yield}	T_{burst}	P_{burst}	P_{final}	T_{lap}	S_{lam}	S_{laf}	T_{rap}	S_{ram}	S_{raf}	T_{cps}	T_{cpf}	CP_s	CP_f
1	14.8	8.4	38.5	42.1	12	32	49.5	11.5	63	97.5	4	14.5	54.5	73.5
2	13.9	9.5	39.3	41.5	10.5	39	49.5	12	62.5	100	4	14	54.5	74.5
3	14.1	10.9	39.3	40.9	10.5	37	48.5	12	65.5	99.5	4	14	54.5	74.5
4	12.3	8.3	36.9	42.6	12	32	50	12	69.5	99	5	15	54	74
5	14.4	8.2	37.6	41.9	12	39	49.5	12	60.5	99.5	4.5	14	54	72.5

Table 16 Comparison between the results of FEA and SA algorithm according to the optimum load paths

No.	SA		Abaqus		Error	
	T(mm)	H(mm)	T(mm)	H(mm)	T	H
1	1.380	52.95	1.391	52.90	0.79	0.11
2	1.398	53.05	1.414	53.64	1.11	1.10
3	1.408	51.87	1.421	52.92	0.90	1.99
4	1.384	52.37	1.401	52.70	1.19	0.62
5	1.390	53.23	1.396	53.52	0.42	0.54

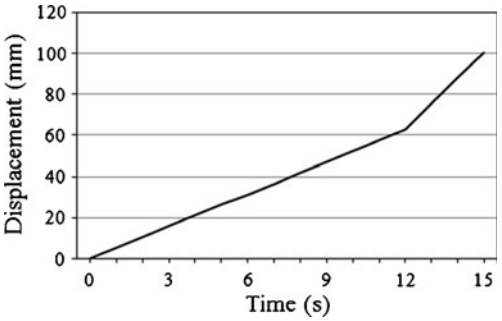

Fig. 34 The optimal path of right axial-punch displacement

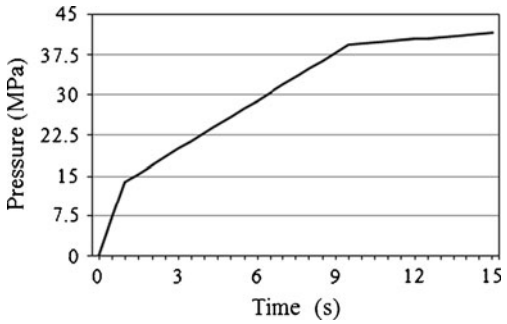

Fig. 32 The optimal path of internal pressure

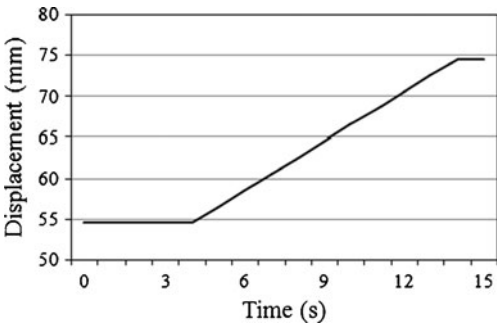

Fig. 35 The optimal path of the counter-punch displacement

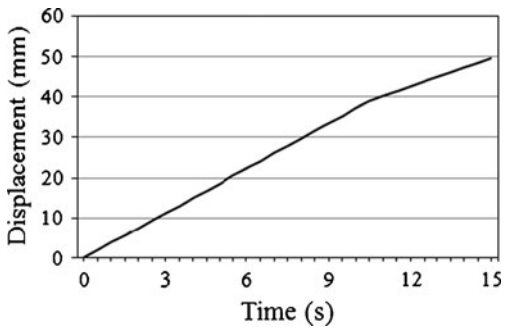

Fig. 33 The optimal path of left axial-punch displacement

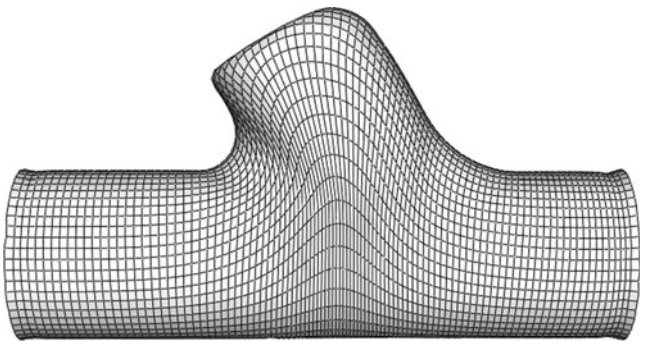

Fig. 36 Tube formed by applying of optimal load paths

observed that the predefined condition is satisfied and the linear model could estimate the tube formability versus loading variables. Now, five sets of arbitrary variables with their respective bounds are considered and the differences between the FEA and regression models are found, see Table 14. It is seen that the differences are negligible and these models can estimate tube formability versus loading variables with an appropriate accuracy. The distribution of real data around the regression line for the minimum thickness using linear model is shown in Fig. 28 and a good conformability is observed. Figure 29 illustrates the effect of load variables on the protrusion height. As it is observed, the total displacement of right axial-punch has a significant effect on the protrusion height. However, ANOVA could help to decrease the number of variables involved in the process that is useful to reduce the complexity of test and production cost. Pairwise effect of the yield pressure (P_{yield}) and the final displacement of right axial-punch (S_{raf}) on the protrusion is seen in Fig. 30 which can help the manufactures to investigate the influence of each variable on the outputs in more detail. Similar to pairwise effect investigation of protrusion height, it can be studied for other load variables.

In this algorithm, an objective function in a form of error function is defined which is constructed as follows;

$$f = \frac{\left(T_{\exp} - T\right)^2}{T_{\exp}} + \frac{\left(H_{\exp} - H\right)^2}{H_{\exp}} \tag{22}$$

where T_{exp} and H_{exp} are calculated by Eqs. 19 and 20, respectively and T and H are desired values defined by the designer. The proposed SA code is written in Matlab and the resultant convergence rate of the algorithm is shown in Fig. 31. Five sets of optimum parameters are calculated and the results are listed in Table 15. The obtained optimal loading parameters based on the SA and FEA results are compared to each other in Table 16. The second set of load variables in Table 15 is selected to design the optimal load paths based on the lower error and high quality of tube formability. The respective load paths for internal pressure, left and right axial-punch displacements, and counter-punch displacement are shown in Figs. 32, 33, 34 and 35, respectively.

The final shape of formed tube attained by the application of optimum load paths is shown in Fig. 36. As it is noticed, the tube has been formed to Y-shape without any defect and has high quality in comparison to the experimental model [4]. The final pressure of Altan study [4], the minimum thickness and the maximum protrusion height of simulation and optimal models are examined here. The final pressure in Altan study is 130 MPa while it is reduced to 41.5 MPa in the current optimal condition. Moreover, the minimum thickness for the simulation and optimum models are 1.14 and 1.414 mm, respectively. Furthermore, the maximum protrusion height in two cases are 46.13, 53.64 mm, respectively. As it is observable, all aforementioned criteria are improved, however, the final pressure is reduced more remarkably (about 32%). Hence, by applying the optimal load paths, a better quality of hydroformed tube with lower capacity of required equipments may be obtained.

Conclusion

An optimization of load paths in hydroforming of X- and Y- tube shapes versus loading parameters are investigated. The optimal conditions for loading variables were determined by using SA algorithm in conjunction with FEA. The ANOVA was used to investigate the instantaneous effect of two variables on the outputs. It is found that using optimal loading parameters cause significant improvement in the quality of final product containing the variance of tube thickness and the height of protrusion. It is also found that the resultant progress may be achieved in spite of lower capacity of required instruments which is an important outcome. The method applied here is seems promising and may be applied to other more complicated tube hydroforming processes.

References

1. Ray P, Mac Donald BJ (2005) Experimental study and finite element analysis of simple X- and T-branch tube hydroforming processes. Int J Mech Sci 192:1498–1518
2. Ray P, Mac Donald BJ (2004) Determination of the optimal load path for tube hydroforming processes using fuzzy load control algorithm and finite element analysis. Finite Elem Anal Des 41:173–192
3. Kocanda A, Sadlowska H (2006) An approach to process limitations in hydroforming of X- joints as based on formability evaluation. J Mater Process Technol 177:663–667
4. Jirathearanat S, Hartl C, Altan T (2004) Hydroforming of Y-shapes-product and process design using FEA simulation and experiments. J Mater Process Technol 146:124–129
5. Ingarao G, Lorenzo RD, Micari F (2009) Internal pressure and counterpunch action design in Y-shaped tube hydroforming processes: a multi-objective optimization approach. Comput Struct 87:591–602
6. Cheng DM, Teng BG, Guo B, Yuan SJ (2009) Thickness distribution of a hydroformed Y- shape tube. Mat Sci Eng A 499:36–39
7. Douglas CM (1996) Introduction to linear regression analysis, Second Edition. John Wiley& Sons, Inc. pp.8-15
8. Kirkpatrick S (1992) Transportation planning and technology. Science 16:261–273

9. Metropolis MC (1996) Simulated annealing and I.E.T. algorithm: theory and experiments. Lmens, 96–21
10. Yingyot AUL, Gracious N, Taylan A (2004) Optimizing tube hydroforming using process simulation and experimental verification. J Mater Process Technol 146:137–143
11. Hwang YM, Lin TC, Chang WC (2007) Experiments on T-shape hydroforming with counter punch. J Mater Process Technol 192–193:243–248
12. Fann KJ, Hsiao PY (2003) Optimization of loading conditions for tube hydroforming. J Mater Process Technol 140:520–524
13. Imaninejad M, Subhash G, Loukus A (2005) Loading path optimization of tube hydroforming process. Int J Mach Tool Manu 45:1504–1514
14. Kashani Zadeh H, Mosavi Mashhadi M (2006) Finite element simulation and experiment in tube hydroforming of unequal T shapes. J Mater Process Technol 177:684–687